Science of the Total Environment 745 (2020) 140932

Contents lists available at ScienceDirect

Science of the Total Environment

journal homepage: www.elsevier.com/locate/scitotenv

The glyphosate formulation Roundup® LB plus influences the global metabolome of pig gut microbiota *in vitro*

Jannike L. Krause [a,1], Sven-Bastiaan Haange [b,1], Stephanie S. Schäpe [b], Beatrice Engelmann [b], Ulrike Rolle-Kampczyk [b], Katarina Fritz-Wallace [b,d], Zhipeng Wang [b], Nico Jehmlich [b], Dominique Türkowsky [b], Kristin Schubert [b], Judith Pöppe [e], Katrin Bote [e], Uwe Rösler [e], Gunda Herberth [a], Martin von Bergen [b,c,*]

[a] Helmholtz-Centre for Environmental Research - UFZ, Department of Environmental Immunology, Leipzig, Germany
[b] Helmholtz-Centre for Environmental Research - UFZ, Department of Molecular Systems Biology, Leipzig, Germany
[c] Institute of Biochemistry, Faculty of Biosciences, Pharmacy and Psychology, University of Leipzig, Germany
[d] National Center for Tumor Diseases - NCT, Dresden, Germany
[e] Institute for Animal Hygiene and Environmental Health, Freie Universität Berlin, Berlin, Germany

HIGHLIGHTS

- The influence of Roundup was investigated at a relevant concentration.
- Microbiota effects were investigated in a colon simulating bioreactor model.
- No discernable effect on community taxonomy and enzymatic repertoire.
- No discernable effect on short-chain fatty acids, amino acids and bile acids.
- Subtle effects were observed on the metabolome.

GRAPHICAL ABSTRACT

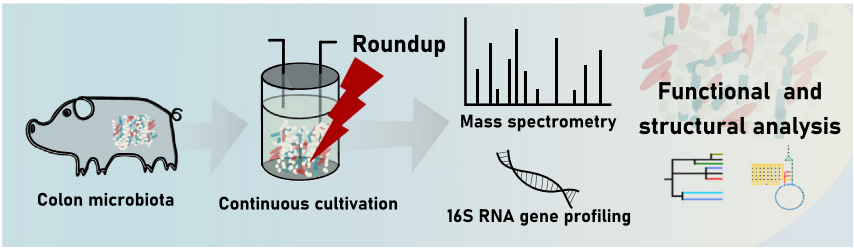

ARTICLE INFO

Article history:
Received 3 June 2020
Received in revised form 6 July 2020
Accepted 11 July 2020
Available online 17 July 2020

Editor: Jay Gan

Keywords:
16S
Metaproteome
Meta-metabolome
Continuous *in vitro* culture
Bioreactor
Microbiome

ABSTRACT

Glyphosate is the world's most widely used herbicide, and its potential side effects on the intestinal microbiota of various animals, from honeybees to livestock and humans, are currently under discussion. Pigs are among the most abundant livestock animals worldwide and an impact of glyphosate on their intestinal microbiota function can have serious consequences on their health, not to mention the economic effects. Recent studies that addressed microbiota-disrupting effects focused on microbial taxonomy but lacked functional information.
Therefore, we chose an experimental design with a short incubation time in which effects on the community structure are not expected, but functional effects can be detected. We cultivated intestinal microbiota derived from pig colon in chemostats and investigated the acute effect of 228 mg/d glyphosate acid equivalents from Roundup® LB plus, a frequently applied glyphosate formulation. The applied glyphosate concentration resembles a worst-case scenario for an 8–9 week-old pig and relates to the maximum residue levels of glyphosate on animal fodder. The effects were determined on the functional level by metaproteomics, targeted and untargeted meta-metabolomics, while variations in community structure were analyzed by 16S rRNA gene profiling and on the single cell level by microbiota flow cytometry.
Roundup® LB plus did not affect the community taxonomy or the enzymatic repertoire of the cultivated microbiota in general or on the expression of the glyphosate target enzyme 5-enolpyruvylshikimate-3-phosphate synthase in detail. On the functional level, targeted metabolite analysis of short chain fatty acids (SCFAs), free amino

* Corresponding author.
E-mail addresses: jannike-lea.krause@ufz.de (J.L. Krause), martin.vonbergen@ufz.de (M. von Bergen).
[1] Authors contributed equally

https://doi.org/10.1016/j.scitotenv.2020.140932

acids and bile acids did not reveal significant changes, whereas untargeted meta-metabolomics did identify some effects on the functional level.
This multi-omics approach provides evidence for subtle metabolic effects of Roundup® LB plus under the conditions applied.

1. Introduction

Since 2015, the debate about possible health risks of glyphosate for humans and livestock has come into the medial focus (Tarazona et al., 2017). Glyphosate-based herbicides are the most frequently used pesticide group worldwide (Benbrook, 2016) with applications ranging from agricultural to non-agricultural applications (Hanke et al., 2010). Consequently, it enters the organisms after the consumption of contaminated food or fodder (Licht and Bahl, 2019; Claus et al., 2016). In humans, but also in cows and rats, glyphosate is primarily taken up *via* the diet (Brewster et al., 1991) and therefore the intestinal microbiota is especially prone to exposure. Glyphosate targets the enzyme 5-enolpyruvylshikimate-3-phosphate synthase (EPSPS) from the shikimate pathway and thus blocks the synthesis of the aromatic amino acids tyrosine, phenylalanine and tryptophan (Amrhein et al., 1980). As only organism group, animals lack the shikimate pathway and thus the EPSPS. Hence, to date glyphosate is considered safe for humans and animals (Myers et al., 2016). Similar to plants, most microorganisms use the shikimate pathway to synthesize aromatic amino acids. Two classes of the EPSPS exist in bacteria: the glyphosate sensitive class I EPSPS (Funke et al., 2009) and the glyphosate insensitive class II EPSPS (Priestman et al., 2005). Glyphosate has antimicrobial properties (US patent 7771736 B2) and thus could potentially affect growth of sensitive species *e.g.* in the intestine. Several studies have investigated the effect of glyphosate acid or glyphosate-based formulations on the intestinal microbiota (Tsiaoussis et al., 2019) *in vivo* and *in vitro* studies at different concentrations and in different species, not surprisingly leading to contrary results.

In vivo studies pose four major challenges when assessing microbiota-modulating effects. First, host effects can distort the conclusions drawn from analyzing the taxonomic or functional parameters of the microbiota (Payne et al., 2012). Second, cage-effects coming from animal housing and exposure in separate treatment groups can facilitate the misinterpretation of results. Third, the characterization of the initial microbiota, to discriminate treatment-related community shifts from normal variation, is often neglected. Fourth, microbiota at different facilities from different animal strains might respond differently (Macpherson and McCoy, 2015). One option to address these challenges is to use *in vitro* cultivation systems with defined cultivation parameters. This allows the long-term cultivation of microbiota and the investigation of acute or chronic microbiota modulating effects coming from the exposure itself (Payne et al., 2012).

Healthy intestinal microbiota shows a high inter-individual taxonomic variability between individual hosts, though they share the same "healthy" functional repertoire (Qin et al., 2010; Turnbaugh et al., 2007). Thus, microbial communities can shift in their distribution of taxa and still exhibit "healthy" functional properties for the host. Consequently, these alterations might be considered neutral, beneficial or harmful, depending on their contribution to a diseased state (Levy et al., 2017; Lozupone et al., 2012). Therefore, concentrating on the functional repertoire is essential to identify non-healthy states (Levy et al., 2017; Lozupone et al., 2012). The effect of glyphosate on microorganisms was investigated *in vitro* on pure bacterial batch cultures from poultry (Shehata et al., 2013) and continuous cultures of bovine rumen microbiota (Riede et al., 2016). However, the latter study primarily focused on taxonomic changes upon glyphosate exposure.

Over the past decade, culture-independent methods like metagenomics, metatranscriptomics, metaproteomics, meta-metabolomics (hereafter metabolomics) and cytomics have been developed to investigate functional and structural properties in microbiota. Metagenomics captures the potential physiology of a microbiota but lacks the discrimination between live and dead cells (Xu, 2006). Even though the metagenome-based prediction of functionality has improved, there is still a great need to verify the potential activity by analyzing the functional activity (Franzosa et al., 2015). Metatranscriptomics allows time-point specific insights into the transcriptional regulation of the microbiota, but still lacks the functional proof (Bashiardes et al., 2016), whereas metaproteomics provides real functional information and furthermore provides information on the taxonomy by analyzing microbial enzymes (Heintz-Buschart and Wilmes, 2018; von Bergen et al., 2013). Metabolomics complements metaproteomics by measuring the metabolites arising from enzymatic activity (Yadav et al., 2018). Cytomics captures microbial community structure variations on the single-cell level by measuring optical characteristics, but does not resolve functional processes performed in individual bacterial cells (Koch et al., 2013).

With our approach, we circumvent possible challenges from *in vivo* exposure and analyze the effects of Roundup® LB plus on continuously cultivated pig colonic microbiota. We analyzed the taxonomic distribution as a baseline analysis and focused on functional effects by the application of a comprehensive multi-omics approach. Therefore, in this study, we acutely exposed pig microbiota to Roundup® LB plus at a reasonable high concentration of 228 mg/d glyphosate equivalents. The species composition was assessed by 16 S rRNA gene profiling and the enzymatic repertoire and the subsequent metabolites by metaproteomics and metabolomics.

2. Materials and methods

2.1. Chemicals and reagents

Acetonitrile, methanol, ammonium acetate and ammonium hydroxide were purchased from Sigma Aldrich (St.Louis, MO, USA). Solvents for mass spectrometry were of analytical grade purity. Experimental water (resistivity 18.2 MΩcm) was purified using a Milli-Q-System (Millipore, Milford, MA, USA).

For *in vitro* exposure of intestinal microbiota, the glyphosate-based herbicide Roundup® LB plus (Monsanto Agrar Deutschland GmbH, PZN 250524, approval number 024142-60) was used. Roundup® LB plus is a mixture of water (42.5%), glyphosate isopropylamine salt (41.5%), and surface-active-ingredient (16%; safety data sheet, MONSANTO Europe, 14.10.2015).

For glyphosate quantitation, a standard stock solution of Roundup® LB plus (10 μg/mL) was prepared in Milli-Q water. Glyphosate (N-(phosphonomethyl)-glycine) was obtained from Glentham Life Sciences Ltd. (Wiltshire, UK). Standard stock solutions (10 μg/mL) were prepared in Milli-Q water and stored at −20 °C. Working dilutions were prepared in Milli-Q-water before use.

2.2. Bioreactor model of pig colonic microbiota

Colon content of two 8 to 9 week old male German Landrace pigs (Landesamt für Gesundheit und Soziales, number H0005/18) was sampled, directly put under anaerobic conditions (AnaeroGen 2.5 L; Thermo Scientific) and stored at −80 °C.

Four parallel and independent 250 mL bioreactor vessels of a Multifors 2 bioreactor system (Infors, Bottmingen Switzerland) were

set-up under anaerobic conditions with sterile complex intestinal medium adjusted to pig (CIM, Supplemental Table 1). Anaerobic conditions were maintained by constant gassing of bioreactor vessels and reservoir bottles with sterile nitrogen. Cultivation temperature was set to 37 °C and pH was adjusted to 6.5 by automatic addition of 1 M sodium hydroxide. Constant stirring at 150 rpm prevented settling of bacteria. The bioreactors were run under experimental conditions for 24 h to prove sterility (sterile run: S, Fig. 1A).

Colon content was thawed anaerobically (37 °C, 60 min) and slurry equal to 1 g colon content was mixed with the double amount of prewarmed CIM. Coarse material was given 2 min of settling and then the whole supernatant was used to inoculate two bioreactors with bacteria suspension from 0.5 g colon content per bioreactor. The community was given 24 h to establish and then continuous cultivation started at a dilution rate of D = 0.02 (residence time of 48 h, (Wilfart et al., 2007)). The communities were cultivated for a total of 25 days. After ten bioreactor turn-over (day 21 ± 1), the bioreactor system were considered to be at steady state (McNeil and Harvey, 2008) and the days 20–22 resemble the control phase. After sampling on day 22, the communities were exposed to Roundup® LB plus. Therefore, Roundup® LB plus war spiked into the bioreactor vessels and supplied with the medium feed to maintain the defined concentration during the treatment phase days 23 to 25 (Fig. 1A).

The applied concentration was chosen on the basis of the calculated maximal dietary burden of 2.85 mg/kg body weight per day recorded by EFSA (Authority, 2018). This value was applied to an 80 kg pig resulting in a daily exposure of 228 mg glyphosate. This study aims to identify microbiota-modulating properties of the frequently applied glyphosate-formulation Roundup® LB plus and hence the amount of 228 mg/d glyphosate-equivalents from Roundup® LB plus (1.8 mg/mL in feed medium) was fed into the bioreactors.

Samples were taken in a multiple of 24 h, starting with an initial sampling after one day and during the control and treatment phase. For 16S rRNA gene profiling, short chain fatty acid (SCFA) analysis, untargeted metabolomics and metaproteomics samples were centrifuged (5000*g*, 5 min, 4 °C). Cell pellets without supernatant were stored directly at −20 °C for 16S rRNA gene profiling and metaproteomics, whereas the supernatants for metabolomics were stored at −80 °C.

2.3. Microbiota flow cytometry

Immediately after sampling, bacteria were pelleted (3200 ×*g*, 10 min, and 4 °C) and preserved in 2% formaldehyde (stock: 8% formaldehyde at pH 7, diluted with PBS (6 mM Na_2HPO_4, 1.8 mM NaH_2PO_4 and 145 mM NaCl in bi-distilled water, pH 7)) at RT for 30 min. Afterward, the bacteria were centrifuged (3200*g*, 10 min, and 4 °C) and fixed in 70% ethanol for long-term storage at −20 °C.

After a minimum of one day at −20 °C, the bacteria were washed with PBS, treated by ultra-sonication, OD adjusted ($OD_{\lambda 700nm}$ ($d_{cuvette}$ = 0.5 cm) = 0.035), treated for 20 min at RT with permeabilization buffer containing 0.11 M citric acid and 4.1 mM Tween20 and stained with 0.68 μM 4′,6-di-amidino-2-phenyl-indole (DAPI, Sigma-Aldrich, St-Louis, USA) overnight in the dark. Measurement and data analysis were performed as in (Krause et al., 2020) except changed neutral density filter for side scatter (ND 1.9). Raw cytometric data and gate templates can be found at flow repository ID: FR-FCM-Z2L4 under: https://flowrepository.org.

2.4. Targeted glyphosate measurements

The analysis of glyphosate and AMPA by LC-MS/MS was done as previously described (Fritz-Wallace et al., 2020). In brief, 10 μL of the

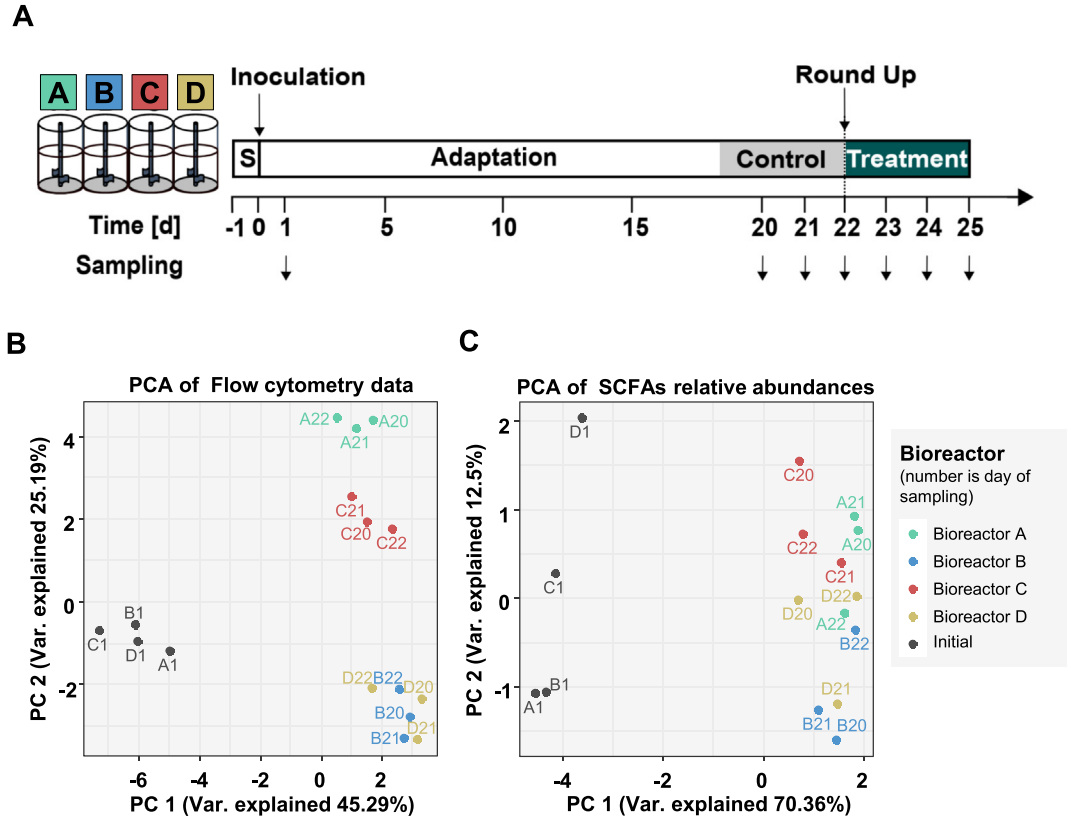

Fig. 1. Experimental setup and analysis of community steady state before Roundup treatment. **A:** After the sterile run (S) all bioreactors A, B, C and D were inoculated with pig colonic microbiota and given time for adaptation. **B:** Whether the communities reached a steady state was determined before treatment by principal component analysis (PCA) of microbiota flow cytometry data and short chain fatty acid abundances.

resuspended extract were injected onto a BEH Amide column (2.1 × 100 mm, 1.7 μm) supplied by Waters (Milford, USA). Chromatographic separation was performed with a gradient of solvent A (66% H_2O, 33% acetonitrile, 10 mM ammonium acetate, 0.04% ammonium hydroxide; pH 9) and solvent B (10% H_2O, 90% acetonitrile, 10 mM ammonium acetate, 0.04% ammonium hydroxide; pH 9). The LC was run at a constant flow rate of 0.4 mL/min. Initial equilibration for 2 min with 0% B, within 2.5 min gradient from 0 to 100% solvent B, hold 100% solvent B for 2 min, back to 0% solvent B for 3.4 min. MRM measurement of glyphosate was done on a QTRAP® 5500 (AB Sciex, Framingham, USA) in negative ionization mode. Data acquisition and analysis were performed in Analyst® Software (AB Sciex, Framingham, USA, version 1.6.2).

2.5. 16 S rRNA gene profiling

Bacteria pellets were thawed and one volume of bacteria slurry was mix with 30 volumes of sterile 10% Chelex (*w*/*v*) solution. After incubation in a ThermoMixer® (Eppendorf, Hamburg, Germany) at 95 °C for 45 min and 1000 rpm shaking samples were centrifuged for 3 min at 11,000*g*. The DNA containing supernatant was transferred into a fresh, sterile tube and stored at −20 °C.

The 16S gene region V3 to V4 was amplified with the primers 341F and 806bR, sequencing was performed on an Illumina MiSeq DNA sequencer (Illumina, San Diego, USA). 16S amplicon generation, sequencing and analysis were done by StarSeq GmbH (Mainz, Germany). Raw data analysis was done by StarSeq GmbH (Mainz, Germany) following their standard data analysis pipeline. Briefly, raw data were demultiplexed, quality checked by FastQC, primers trimmed. Paired-end reads were joined, low-quality reads were removed reads were corrected, chimeras removed and Amplicon Sequence Variants (ASVs) were obtained by the deblur workflow. Taxonomy was annotated to the ASVs using the SILVA 138 database (Quast et al., 2013). The reads counts per ASV with taxonomic annotation were normalized, by dividing the read counts by sum of sequence in the given sample and multiplying by the minimum sum across all samples using the R scripts from Rhea (Lagkouvardos et al., 2017). In addition, relative abundances of each ASV and taxa were calculated using Rhea (Lagkouvardos et al., 2017)

2.6. Metaproteomics

As described previously (Schape et al., 2019), thawed bacteria pellets were dissolved in the 1000 μL lysis buffer (10 mM Tris-HCl, NaCl 2 mg/mL, 1 mM PMSF, 4 mg/mL SDS). For cell disruption following steps were applied: 1. Bead beating (FastPrep-24, MP Biomedicals, Santa Ana, USA: 5.5 ms, 1 min, 3 cycles), 2. 15 min incubation at 60 °C (Thermomixer comfort 5355, Eppendorf, Germany) and 3. Ultrasonication (UP50H, Hielscher, Teltow, Germany; cycle 0.5, amplitude 60%). The protein concentrationwas determined with bicinchoninic acid assay according to the manufacturer's instructions (Pierce™ BCA Protein Assay Kit, Thermo Fisher Scientific, Waltham, USA). 100 μg protein was precipitated in acetone 1:5 (*v*/v) at −20 °C overnight and then centrifuged (10 min, 14,000×g). The precipitate was dissolved in Laemmli buffer and used for SDS-PAGE analysis, in-gel digestion and protein purification with ZipTip® treatment (Haange et al., 2019).

Five μg peptide lysate were injected into nanoHPLC (UltiMate 3000 RSLCnano, Dionex, Thermo Fisher Scientific, Waltham, USA). Peptides were separated on a C18 reverse-phase trapping column (C18 PepMap100, 300 μm × 5 mm, particle size 5 μm, nano viper, Thermo Fischer Scientific, Waltham, USA), followed by a C18 reverse-phase analytical column (Acclaim PepMap® 100, 75 μm × 25 cm, particle size 3 μm, nanoViper, Thermo Fisher Scientific, Waltham, USA). Mass spectrometric analysis of peptides was performed on a Q Exactive HF mass spectrometer (Thermo Fisher Scientific, Waltham, USA) coupled to a TriVersa NanoMate (Advion, Ltd., Harlow, UK) source in LC chip coupling mode. LC gradient, ionization mode, and mass spectrometry mode are described elsewhere (Haange et al., 2019). Raw data were processed with Proteome Discoverer (vr2.2, Thermo Fischer Scientific, Waltham, USA). Search settings for the Sequest HT search engine were set to: trypsin (full), max. Missed cleavage: 2, precursor mass tolerance: 10 ppm, fragment mass tolerance: 0.02 Da. Protein grouping was enabled, with protein group requiring at least one unique peptide. For complex microbiota, protein-coding sequences of all bacteria were downloaded from UniProt (13.05.2017; http://www.uniprot.org/) resulting in 15,214,675 protein-coding sequences. Protein identification was performed as descried in (Schape et al., 2019).

2.7. Untargeted metabolomics

Supernatants were thawed at 37 °C for 5–10 min. For metabolites extraction, five volumes of methanol:acetonitrile:water (2:3:1) were added to the supernatant and samples were vortexed for 5 min. Afterwards, the samples were sonicated for 5 min and centrifuged at 18000 ×*g* for 5 min. Supernatants were transferred into fresh tubes and dried under vacuum (SpeedVac™, Eppendorf, Hamburg, Germany). Dried pellets were resuspended in 100 μL of a 1:1 mix of running solvent A (0.1% formic acid in water) and B (2% isopropanol, 0.1% formic acid in acetonitrile).

10 μL extract was injected into an HPLC-QToF instrument from Agilent Technologies (6540 UHD Accurate-Mass Q-TOF LC/MS instrument) for LC-MS/MS measurement. Metabolites were separated on a C18 column (flow rate: 0.3 mL/min) with the following gradient of running solvent A, and running solvent B: 0–5.5 min 1% B, 5.5–20 min 1%–100% B, 20–22 min 100% B, 22.-22.5 min 100%–1% B and 22.5–25 min 1% B. The QToF was set up in centroid mode and in screening mode allowing the detection of ions with a mass to charge ratio between 60 and 1000. After a full scan, the most intense ion (threshold 200 counts) was fragmented.

Raw files (.d) were imported into Progenesis QI 2.1 software (Waters, Milford, USA). Different ionization modes were processed separately. Isotope and adduct fusion were applied and covered $[M + H]^+$, $[M + ACN + H]^+$, $[M + H\text{-}H2O]^+$ in positive mode and $[M\text{-}H]^-$, $[M\text{-}H20\text{-}H]^-$ for negative mode, respectively. The next steps included alignment of ion chromatograms in t_R direction based on a reference chromatogram chosen automatically from the data set. The following peak picking was done using default sensitivity settings. Database search was performed using ChemSpider as identification method with *E. coli* metabolome database, fecal metabolome database and KEGG as input selection. Precursor and fragment mass tolerance were set to 20 ppm and 10 ppm, respectively. Only precursor peaks with corresponding fragment spectra were kept. Normalized peak areas and possible identifications were exported. For quality control purposes, peaks detected in medium and medium with added Roundup® LB plus were excluded from the corresponding samples (D1-D22: medium; D23-D25: medium with added Roundup® LB plus). Samples were grouped according to their treatment with Roundup® LB plus. Only peaks with valid values in at least 50% of replicates in both groups were considered for further analysis.

2.8. Targeted bile acid analysis

Bile acids were quantified as previously described (Haange et al., 2020). Briefly, for bile acid measurements the bile acids kit (Biocrates Life Sciences AG, Innsbruck, Austria) was used as outlined in the manufacturer's instructions. In short, 10 μL samples were used for the assay on a 96-well plate format. All isobaric bile acids were separated by HPLC, with a flow rate of 0.4 mL/min and at a column pressure of 400 bar. The HPLC runtime was 11 min. Eluting bile acids were measured online with a triple quadrupole mass spectrometer (MS/MS) using an electrospray source in negative mode. For the quantitation, a calibration set with seven concentration levels and a mixture of 10 internal standards was used (Siskos et al., 2017).

2.9. Targeted short-chain fatty acids (SCFA) analysis

As described previously (Schape et al., 2019), supernatants were thawed at 37 °C for 5–10 min. The samples were mixed with acetonitrile to a final concentration of 50% acetonitrile. SCFAs were derivatized for 30 min at 40 °C with 0.5 volumes of 200 mM 3-nitrophenylhydrazine and 0.5 volumes 120 mM N-(3-dimethylaminopropyl)-N'-ethylcarbodiimide hydrochloride in pyridine. For LC-MS/MS measurement, the mix was diluted 1:50 in 10% acetonitrile.

50 μL diluted SCFA derivatives were injected into the LC-MS system. SCFAs were separated on an Acquity UPLC BEH C18 column (1.7 μm) (Waters, Milford, USA) with solvent A: 0.01% formic acid in water and solvent B: 0.01% formic acid in acetonitrile as mobile phases. The column flow rate was set to 0.35 mL/min, the column temperature to 40 °C. The gradient elution was done as follows: 2 min at 15% solvent B, 15–50% B in 15 min, then held at 100% solvent B for 1 min. Subsequently, the column was equilibrated for 3 min at 15% solvent B. For identification and quantitation, a scheduled Multiple Reaction Monitoring method was used, with specific transitions for every SCFA. Peak areas were determined in Analyst software and areas for single SCFAs were exported. Normalization and statistics were done in R.

2.10. Targeted analysis of amino acids

Free physiological amino acids were quantified on day 1 and day 22 before Roundup® LB plus treatment and on day 23 to 25 during exposure of the bacteria in all bioreactors. Therefore, 100 μL of culture supernatant and blank medium were used for metabolite extraction.

The extraction of amino acids was carried out according to the user guide of EZ:faast kit (KH0-7337, Phenomenex, US). Briefly, seven concentration points (0, 10, 20, 50, 100, 150, 200 nmol/mL) of standard amino acids from SD1 and SD2 were used for calibration. Both of the standards and samples were mixed with 100 μL internal standards, followed by solid-phase extraction, derivatization, and liquid/liquid extraction. The samples were re-dissolved in 100 μL of a 1:1 mix of solvent A/solvent B (solvent A: 10 mM ammonium formate in water, solvent B: is 10 mM ammonium formate in methanol). The derivatized amino acids were analyzed by MRM method on a QTRAP 5500® instrument (AB Sciex, Framingham. USA) after separation on an EZ:faast AAA-MS column (250 × 2.0 mm) with a 17 min gradient at a flow rate of 0.25 mL/min as suggested in the manual.

The data analysis was carried out in the Analyst software (AB Sciex, Framingham, USA, version: 1.6.2). Briefly, the intensity of amino acids from both the standards and samples were normalized by the internal standard intensity. Linear regression curves were calculated on each standard amino acid. To improve the reliability, four replicates of each standard amino acid were used to generate the regression curve to calculate the concentration of amino acids in the samples.

2.11. Statistical analysis of omics data

Alpha-diversity, principal component analysis (PCA) and non-metric multi-dimensional scaling (NMDS) dissimilarity analysis were done in R (Ihaka and Gentleman, 1996) using the basic functions and the vegan package (Dixon, 2003). Statistics were done in R using in-house written scripts as previously described (Haange et al., 2020). Briefly, the statistical tests used were for complete sample data analysis PERMANOVA using the adonis function in the vegan R package (Dixon, 2003), and for single variables Kruskal-Wallis group test followed by a posthoc pairwise Dunn test. Where appropriate (number of tests >20), *P*-values were corrected for multi-testing by the Benjamini-Hochberg method (Benjamini and Hochberg, 1995). K-means were calculated in R using the kmeans function. Heatmaps were constructed with pheatmap R package and all other figures were constructed using the R package ggplots2 (Wickham, 2011).

3. Results

3.1. Microbial communities reached steady state before exposure to Roundup® LB plus

Four pig colonic microbiota (A to D) were cultivated under anaerobic conditions in continuous bioreactors (Fig. 1A). Since it was shown before that the functional and the taxonomic level of microbial communities can develop independently during adaptation or upon perturbation (Krause et al., 2020; Liu et al., 2018), we assessed community development during the control phase per bioreactor on the structural and functional level, respectively. Structural development was determined by microbial flow cytometry (Fig. 1B), depicting bacterial cell division and growth states. Functional development was examined by SCFA analysis (Fig. 1C), which are the main fermentation products of the intestinal microbiota. After ten full medium exchanges (day 21 ± 1), the communities did not change considerably with regard to both community structure and function. However, flow cytometric analysis of the microbial community indicated differences in the community on the taxonomic level.

We defined a three-day control phase (day 20 to day 22) before Roundup® LB plus treatment and thereafter exposed the microbial communities to 228 mg/d glyphosate acids equivalent during the treatment phase from day 23 to day 25 (Fig. 1A).

3.2. Exposure to Roundup® LB plus did not affect taxonomic community composition

To assess influences of Roundup® LB plus treatment on the community structure of the microbiota, we conducted 16S rRNA gene profiling. Previously, it has been shown that *in vitro* model systems can reveal effects of toxins on the microbiota in short time frames, which would only be observed after weeks in animal models (Li et al., 2019).Compared to the initial communities (day 1) the alpha diversity (Fig. 2A, Shannon effective) increased ($P = 0.0124$). Roundup® LB plus exposure (days 23, 24 and 25) did not alter the microbial alpha diversity compared to the steady-state microbiota in the control phase (days 20, 21 and 22). This was also true for the species richness based on ASV numbers (Supplemental Fig. 1A) and the evenness (Supplemental Fig. 1B).

NMDS dissimilarity analysis was performed on the ASV level to determine global taxonomic differences between samples. As already indicated by microbial flow cytometry, the microbial communities clustered according to the bioreactors from which they originated (Fig. 2B, PERMANOVA $P = 0.001$). However, the communities did not cluster according to whether they were exposed to Roundup® LB plus or not and showing no or little effect on the taxonomic community composition. For a more in-depth look, we analyzed the microbial family distribution. The communities on day 1 from the same inoculum (communities A + B *vs.* communities C + D) were very similar (Fig. 2C). In the initial communities A and B, *Enterobacteriaceae* were the most relative abundant family on day 1, followed by *Lactobacillaceae*, *Bifidobacteriaceae* and *Coriobacteriaceae,* with other families only making up a minor part of the communities. In the initial communities C and D, the most abundant families were *Enterobacteriaceae*, *Lactobacillaceae*, *Lachnospiraceae* and *Bifidobacteriaceae*. During the adaptation phase, the family distribution changed considerably, resulting in the development of four different microbial communities A, B, C and D. On day 20 to 22, the most relative abundant families in all communities were in the order of abundance *Ruminococcaceae*, *Lachnospiraceae*, *Enterobacteraceae* and *Prevotellaceae* (Fig. 2C) though in community B and D *Prevotellaceae* were scarce. In the communities C and D *Bacteroidaceae* were one of the most prominent families. The mean relative distribution of bacterial families of all four communities showed no significant Roundup® LB plus associated shifts on day 23 to day 25. In order to identify smaller effects

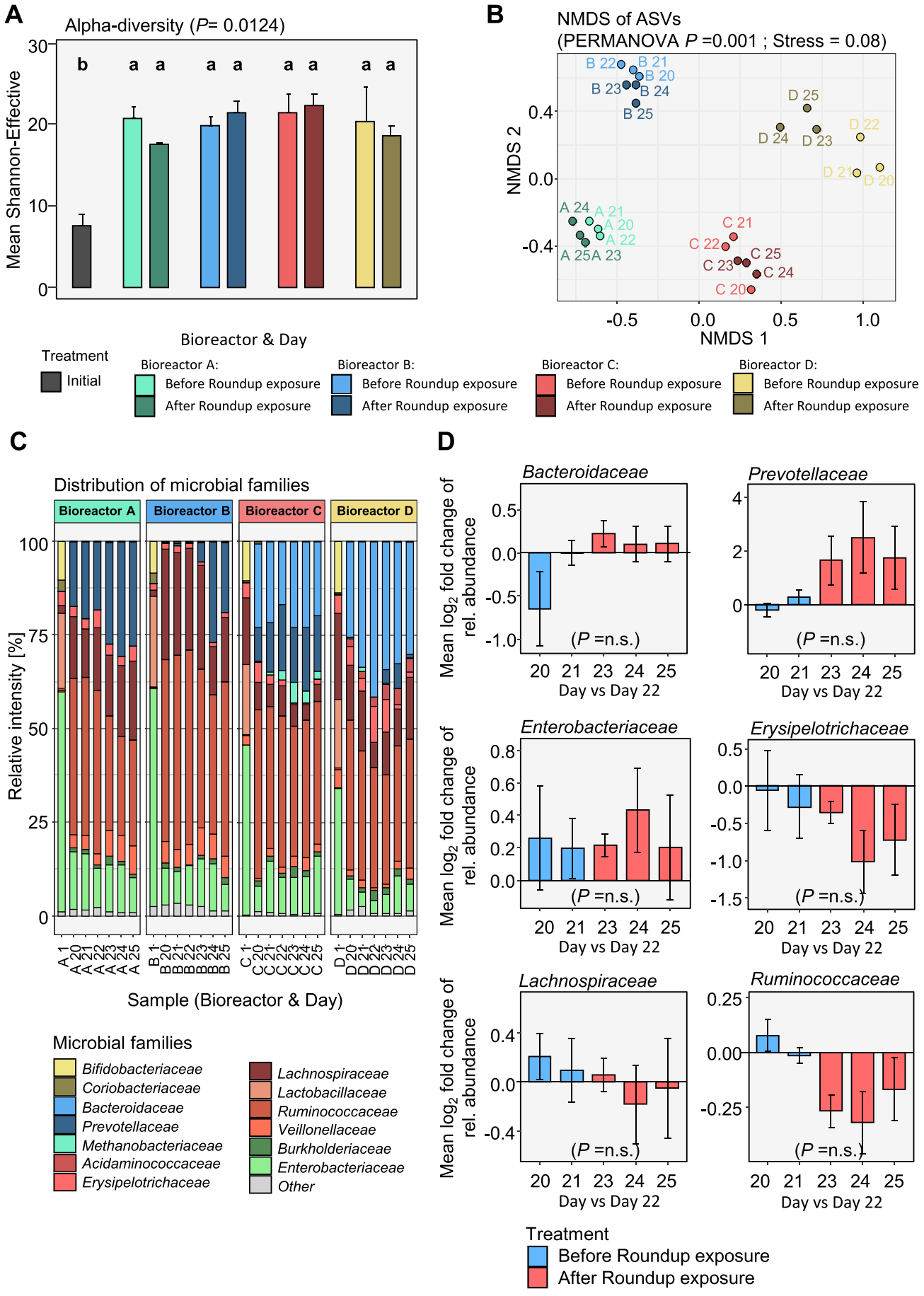
A
Alpha-diversity (P= 0.0124)
Mean Shannon-Effective
b a a a a a a a a
Bioreactor & Day
B
NMDS of ASVs
(PERMANOVA P =0.001 ; Stress = 0.08)
NMDS 1
NMDS 2
Treatment
Initial
Bioreactor A:
Before Roundup exposure
After Roundup exposure
Bioreactor B:
Before Roundup exposure
After Roundup exposure
Bioreactor C:
Before Roundup exposure
After Roundup exposure
Bioreactor D:
Before Roundup exposure
After Roundup exposure
C
Distribution of microbial families
Bioreactor A
Bioreactor B
Bioreactor C
Bioreactor D
Relative intensity [%]
Sample (Bioreactor & Day)
Microbial families
Bifidobacteriaceae
Coriobacteriaceae
Bacteroidaceae
Prevotellaceae
Methanobacteriaceae
Acidaminococcaceae
Erysipelotrichaceae
Lachnospiraceae
Lactobacillaceae
Ruminococcaceae
Veillonellaceae
Burkholderiaceae
Enterobacteriaceae
Other
D
Bacteroidaceae
Prevotellaceae
Enterobacteriaceae
Erysipelotrichaceae
Lachnospiraceae
Ruminococcaceae
Mean log2 fold change of rel. abundance
(P =n.s.)
Day vs Day 22
Treatment
Before Roundup exposure
After Roundup exposure

of Roundup® LB plus on individual families of intestinal microbiota independent of the bioreactor, we calculated the fold change of family abundances compared to the last day of the control phase (day 22) for each of the respective bioreactor. No significant increase or decrease in fold change of the six most abundant microbial families could be detected due to Roundup® LB plus (Fig. 2D). A shift in the ratio of Bactoidetes to Firmicutes has previously been decribed as an indicator for dysbiosis. (Yan et al., 2011; Joly et al., 2013). Therefore similar to above, we calculated the fold-change of the Bacteroidetes to Firmicutes ratio between each day to day 22, and no significant shift was observed for this fold change before and after Roundup-exposure (Supplemental Fig. 1C).

3.3. Roundup® LB plus did not influence the active enzymatic repertoire

Metaproteomics analysis is based on protein content, which quickly responds to changes within one hour (Shamir et al., 2016). Thus, this method analyzes the active enzymatic repertoire of microbial communities and determines taxa distribution, highlighting the metabolic more active taxa (Kleiner et al., 2017).

On the functional active taxonomic level, 50% of the relative intensity was due to protein groups annotated as heterogeneous (Fig. 3A). Heterogeneous protein groups are classified as bacterial proteins but cannot be annotated to a single bacterial family. Mostly this happens because of conserved protein sequence regions between taxa. The relative intensity of protein groups, which could be attributed to specific bacterial families (Fig. 3A), followed the profile of 16S rRNA gene sequencing data (Fig. 2C) to a close degree. Following our expectations and the results from 16S rRNA gene profiling, metaproteomics revealed no influence of Roundup® LB plus on the taxonomic distribution in the microbial communities.

Following this, metaproteomics data were used to reveal the functional repertoire of the microbial communities. The NMDS dissimilarity analysis revealed no global influence of Roundup® LB plus on the metabolic pathways of the communities (Fig. 3B). A more detailed view revealed that the communities A to D possessed a very similar enzymatic repertoire, based on observed KEGG subroles (Fig. 3C). The most prevalent KEGG subroles were *carbohydrate metabolism* followed by *translation*, *energy metabolism*, *transport and catabolism* as well as *amino acid metabolism*. These subroles showed no discernable effect due to the exposure. To ascertain that the general KEGG subrole did not overlook effects, we analyzed in more detail individual KEGG metabolic pathways. Here we concentrated on the amino acid pathways, since glyphosate inhibits aromatic amino acid synthesis *via* the shikimate pathway (Fig. 3D). As above, for each community we looked at the fold changes compared to day 22, just before Roundup-exposure, to remove the variation from the individual bioreactor communities. We neither observed significant effects of Roundup-exposure on the fold changes of amino acid-related enzymes in general nor on enzymes involved in the synthesis of aromatic amino acids, arginine or lysine synthesis (Fig. 3D). Furthermore, the 5-enolpyruvylshikimate-3-phosphate synthase (EPSPS), the enzyme specifically inhibited by glyphosate, did not alter in fold change after Roundup-exposure (Fig. 3D).

3.4. Roundup® LB plus had a slight influence on the metabolome of the microbiota

Since neither the taxonomic community structure nor the enzymatic repertoire of the microbial communities revealed any significant influence of Roundup-exposure, we analyzed the metabolome of the microbiota. Metabolomics is very sensitive and able to detect small functional changes upon stress, though is not able to pinpoint these to specific taxa (Mumtaz et al., 2017).

Since short chain fatty acids (SCFAs) are the major metabolite group produced by the intestinal microbiota and are essential for the host, we decided to perform a targeted analysis of nine SCFAs. The SCFA profile of each community changed between day 1 and the later days (day 20–25) but was not altered by Roundup-exposure (days 20–22 *vs.* days 23–25, Fig. 4A). We additionally analyzed the fold changes of absolute SCFA concentrations per bioreactor individually and plotted the mean and standard deviation. Our analysis revealed no significant effect of Roundup-exposure on SCFA abundances (Fig. 4B).

Following SCFA analysis, we performed untargeted metabolomics on the microbial communities' culture supernatant to capture global effects on the metabolome. We filtered for peaks, which were observed before and after Roundup exposure, to remove peaks attributed to the different Roundup® LB plus constituents. After this filtering, we included 104 peaks for NMDS analysis. NMDS dissimilarity analysis showed a significant shift in the metabolite profile between before (day 20–22) and after (day 23–25) Roundup-exposure, though the metabolite profiles seemed to also cluster by bioreactor (Fig. 4C). A more detailed look at the untargeted metabolome before and after Roundup-exposure revealed a clustering of community peak intensities by bioreactor and, interestingly, by exposure (Fig. 4D). To pinpoint these specific changes in the untargeted metabolic measurements, we did a k-means clustering analysis on the filtered peaks (Fig. 5A). We were able to identify two clusters with responding metabolite profiles (Fig. 5B, clusters 1 and 2). The 16 peaks from the first cluster (Fig. 5B, purple) exhibited an increase in peak intensity after Roundup-exposure, thereby encompassing compounds with higher abundance after Roundup-exposure. The second cluster (Fig. 5B, turquoise), including 16 peaks, showed a decrease in peak intensity and therefore a lower abundance of the corresponding compounds after Roundup-exposure. We were able to annotate several peaks from the two clusters. In cluster 1, one peak was putatively identified as pyridoxamine, a form of vitamin B6, and a second as imidazolepropionic acid, a histidine intermediate. In cluster 2, we were able to putatively annotate one peak to cholic acid (CA), a bile acid. This finding led us to conduct an in-depth targeted analysis of bile acids. We were able to identify and quantify 12 bile acids (Supplemental Table 8). Interestingly, based on fold change analysis to day 22, we found a hint ($P = .0885$) that CA increased after the first day (day 23) of Roundup-exposure and then decreased on the third day (day 25) (Fig. 5C).

3.5. The microbial communities did not metabolize glyphosate in Roundup® LB plus

To check whether glyphosate is metabolized by the microbiota and therefore potentially loses its inhibitory properties on the biosynthesis of aromatic amino acid pathways we determined the concentration of glyphosate in the media. Our targeted measurements revealed no glyphosate in the samples before Roundup-exposure, which was expected, and no change in the concentration of glyphosate in the communities during Roundup-exposure compared to the media provided. This indicates that glyphosate was not metabolized by the microbiota (Fig. 6A).

Fig. 2. 16S rRNA gene profiling data. **A**: Alpha-diversity of the microbiota on ASV level by bioreactor and treatment phase. When Krustal-Wallis test is significant then bars labelled with different letters are significantly to each other ($P < 0.05$). **B**: Beta diversity based on non-metric multidimensional scaling (NMDS) of samples before and after Roundup exposure. Sample names: Letter represents the bioreactor and the number the sampling day. *P* calculated by PERMANOVA. **C:** Relative distribution of microbial families at each sampling day. **D:** Mean $\log_2$ fold changes of relative abundance of selected bacterial families from each sampling day to day 22 (directly before Roundup exposure). Error is SEM, *P* calculated by Kruskal-Wallis with pairwise posthoc test done by Dunn test, n.s. non-significant.

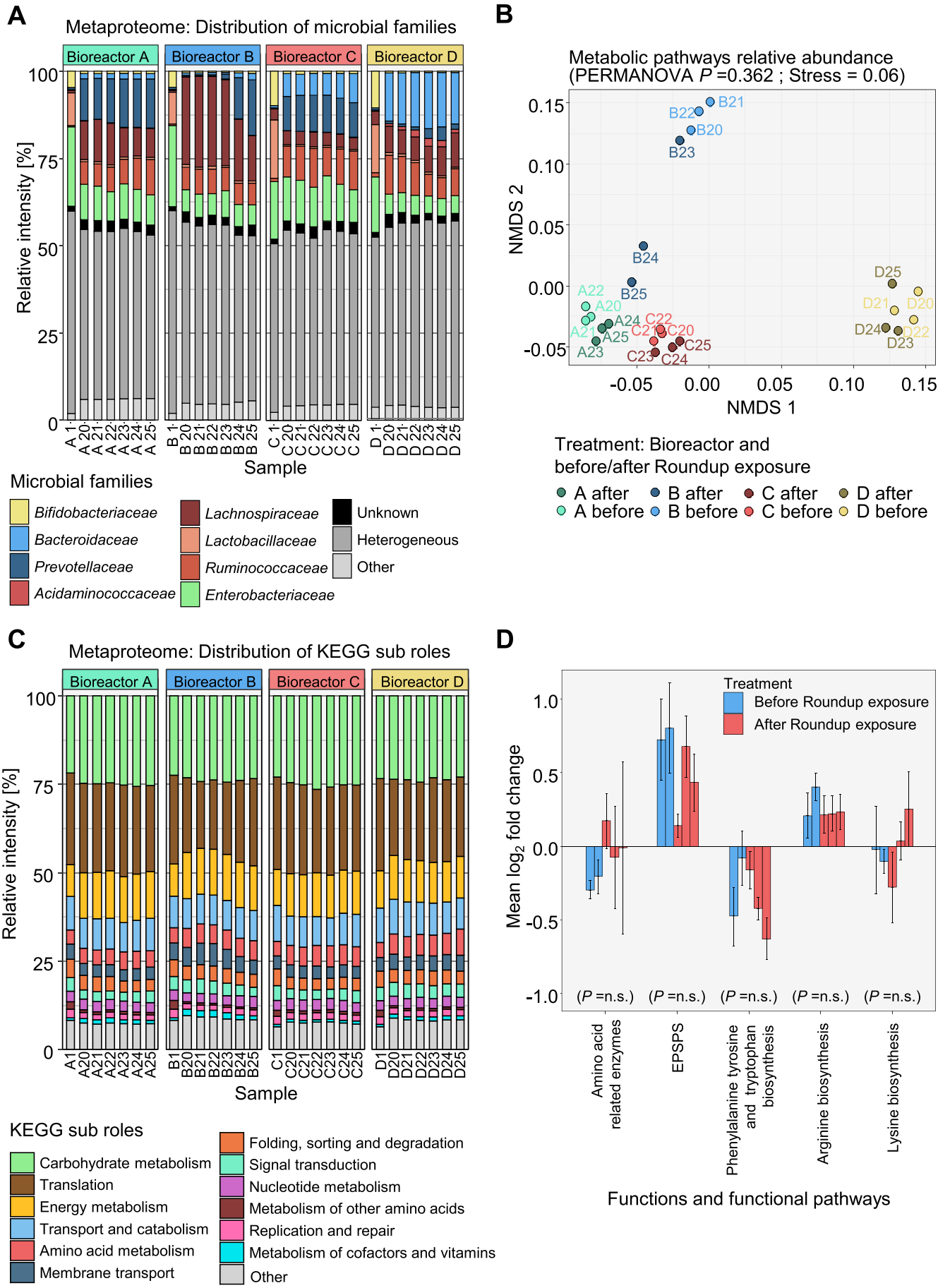
A
Metaproteome: Distribution of microbial families
Bioreactor A
Bioreactor B
Bioreactor C
Bioreactor D
Relative intensity [%]
Sample
Microbial families
Bifidobacteriaceae
Bacteroidaceae
Prevotellaceae
Acidaminococcaceae
Lachnospiraceae
Lactobacillaceae
Ruminococcaceae
Enterobacteriaceae
Unknown
Heterogeneous
Other
B
Metabolic pathways relative abundance
(PERMANOVA P =0.362 ; Stress = 0.06)
NMDS 1
NMDS 2
Treatment: Bioreactor and
before/after Roundup exposure
A after
B after
C after
D after
A before
B before
C before
D before
C
Metaproteome: Distribution of KEGG sub roles
Relative intensity [%]
Sample
KEGG sub roles
Carbohydrate metabolism
Translation
Energy metabolism
Transport and catabolism
Amino acid metabolism
Membrane transport
Folding, sorting and degradation
Signal transduction
Nucleotide metabolism
Metabolism of other amino acids
Replication and repair
Metabolism of cofactors and vitamins
Other
D
Treatment
Before Roundup exposure
After Roundup exposure
Mean log2 fold change
(P =n.s.)
Amino acid related enzymes
EPSPS
Phenylalanine tyrosine and tryptophan biosynthesis
Arginine biosynthesis
Lysine biosynthesis
Functions and functional pathways

3.6. The concentration of aromatic amino acids in the microbial communities did not change after Roundup® LB plus exposure

A reason for the lack of influence of Roundup® LB plus on the microbial communities could be that there is a sufficiently high concentration of aromatic amino acids present in the culture medium. This would negate the need for their synthesis by the microbes. A targeted measurement of amino acids in the medium and in the microbial community samples revealed that aromatic amino acid concentrations were high in pure medium and were being utilized from the medium during cultivation (Supplemental Fig. 2). An NMDS analysis of amino acid concentrations at days 20–25 did not reveal any clustering by Roundup-exposure (Fig. 6B). Furthermore, no significant change in the concentration of tryptophan (Fig. 6C), phenylalanine (Fig. 6D) and tyrosine (Fig. 6E) after Roundup-exposure was observed. This was also true for all other measured amino acids (Supplemental Table 5).

Between days 20 and 25, average aromatic amino acid concentration for each bioreactor was lowest for tryptophan followed by tyrosine, while the concentration of phenylalanine was at least a factor of ten higher (Table 1.)

4. Discussion

Several studies have investigated the effect of glyphosate exposure on the intestinal microbiota *in vitro* and *in vivo* using different organisms. Likewise, from the *in vivo* studies, preferentially using rats, and from the *in vitro* studies the results are contrasting (Riede et al., 2016; Nielsen et al., 2018; Lozano et al., 2018). Furthermore, most of these studies focused on glyphosate-related taxonomic changes, with only two studies analyzing community function at all. Riede et al. (2016) did not identify adverse effects on the ruminal metabolism (Riede et al., 2016). Mesnage et al. (2019, non-reviewed preprint), on the contrary, observed taxonomic changes in the rat caecal microbiota combined with an increase in intermediate metabolites from the shikimate pathway (Mesnage et al., 2019). Because contrasting results shape the debate of potential risks coming from glyphosate exposure, we sought to investigate the microbiota-modulating effects of the most frequently used glyphosate formulation Roundup® LB plus on the function of intestinal microbiota in more detail, using a high concentration. The pig microbiota is an interesting model system because on the one hand, pigs are a livestock species with economic relevance and on the other hand, the pig microbiota is more similar to humans than the intestinal microbiota of other model organisms, such as rodents (Roura et al., 2016). Consequently, analyzing the microbiota-modulating effects of glyphosate on the pig microbiota allows the extrapolation to the human microbiota.

The complex intestinal culture medium in our study was adapted to the pig colon environment (Krause et al., 2020; Tanner et al., 2014). It is well known that microbiota quickly respond to a perturbation on the functional level (Medicine Io, 2003) and, if pressure is high enough, also by shifting towards another stable taxonomic community state (Levy et al., 2017). Therefore, we acutely exposed the microbiota to a high glyphosate concentration by the addition of Roundup® LB plus. However, adult pigs weight over 100 kg, which is associated with a higher fodder uptake and consequently a higher exposure to glyphosate.

The effect of Roundup-exposure in the concentration applied in this study was only slight. Though, these effects cannot singularly be attributed to glyphosate, since Roundup® LB plus contains 16% unknown surface active ingredients. In addition, our data indicate that the colonic microbiota did not metabolize glyphosate. Roundup-exposure neither changed the community taxonomic structure nor the enzymatic repertoire of the microbiota within the three days of exposure. Furthermore, neither the concentration of SCFAs, main products of microbial metabolism, nor the concentration of any of the 29 analyzed amino acids was altered**.** However, a few metabolite peaks were detected at altered abundance by untargeted metabolomics after Roundup-exposure. Of these, only a minority could be annotated to putative compounds, with one peak annotated to cholic acid. The targeted bile acid measurement did show a trend in the decrease in cholic acid after Roundup-exposure. Certain members of the intestinal microbiota are known to deconjugate or dehydroxylate bile acids, and thereby enhancing their toxicity toward other bacteria (Islam et al., 2011; Yokota et al., 2012). Moreover, converted bile acids are involved in signaling between microbiota and host. Alterations to the bile acid profile were reported to affect the metabolism of the host *via* the farnesoid X receptor (Ryan et al., 2014), which controls bile acid synthesis but also glucose and lipid metabolism in the liver. The liver was observed to be one of the major targets affected by ultra-low dose of glyphosate in a two-year study on rats, exhibiting lipotoxic stress and further biochemical and anatomical damage (Mesnage et al., 2015).

The observed metabolic alterations, which did not correspond to significant changes on the proteome level, can be explained by two arguments. First, the metaproteome coverage might not be sufficient for detecting the changes, which might result from rather high community complexity. We have recently shown that community complexity is the most crucial factor determining proteome coverage in metaproteomics (Lohmann et al., 2020). Second, glyphosate or other compounds in Roundup® LB plus, including surfactants, which could possibly harm the intestinal bacteria (Mesnage and Antoniou, 2017) might interfere with other enzymes than the primary target EPSPS. The mode of action of glyphosate is based on its structural similarity to phosphoenolpyruvate (PEP), the physiological substrate of EPSPS. Both compounds compete for EPSPS binding. However, PEP is involved in many other important metabolic processes, such as glycolysis, gluconeogenesis, the synthesis of secondary metabolites or the phosphotransferase sugar uptake system (Kanehisa and Goto, 2000). Thus, the interference by glyphosate could be even broader, as already suggested by a recent study of Ford et al. (2017).

Thermal proteome profiling (TPP) would be a powerful tool to screen the proteome more specifically for proteins interacting with glyphosate (and its metabolites), degrading it or being adversely affected. In the past, this method identified off-targets of active ingredient of drugs (Savitski et al., 2014), but also pollutant degrading enzymes and regulators thereof in bacteria (Türkowsky et al., 2019). TPP might open up a new, interesting perspective for testing of pesticides for health and environmental safety in general.

The contradictory findings of *in vivo* studies might result from a low lab-to-lab reproducibility that derives from the existence of different microbiota in the housing facilities (Hugenholtz and de Vos, 2018) and the different experimental procedures and glyphosate formulations. *E.g.*, Dechartres et al. (2019) daily fed rat dams 5 mg/kg body weight per day glyphosate isopropylamine salt or glyphosate equivalents from Roundup® 3Plus for 30 days and investigated the maternal behavior and neuroplasticity in the hippocampus. However, they barely observed significant effects on maternal behavior or the neurological end-points investigated in their study. In contrast to glyphosate isopropylamine salt, Roundup® 3Plus significantly altered the taxonomy of the intestinal microbiota in their study, indicating that substances from the formulation applied in their study might be causative

Fig. 3. Metaproteomics data. **A**: Distribution of microbial families based on summed measured relative intensities of protein groups assigned to the family. Heterogeneous: protein groups assigned to multiple microbial families. **B:** Beta-diversity of samples by NMDS dissimilarity analysis based on relative abundance of KEGG metabolic pathways. **C:** Distribution of KEGG metabolic subroles based on summed measured relative intensities of protein groups assigned to the family. **D:** Mean $\log_2$ fold changes of summed relative protein group intensities assigned to 5-enolpyruvylshikimate-3-phosphate synthase (EPSPS) and selected amino acid metabolic pathways from each sampling day to day 22 (directly before Roundup exposure). Error is SEM, *P* calculated by Kruskal-Wallis with pairwise posthoc test done by Dunn test, n.s. non-significant.

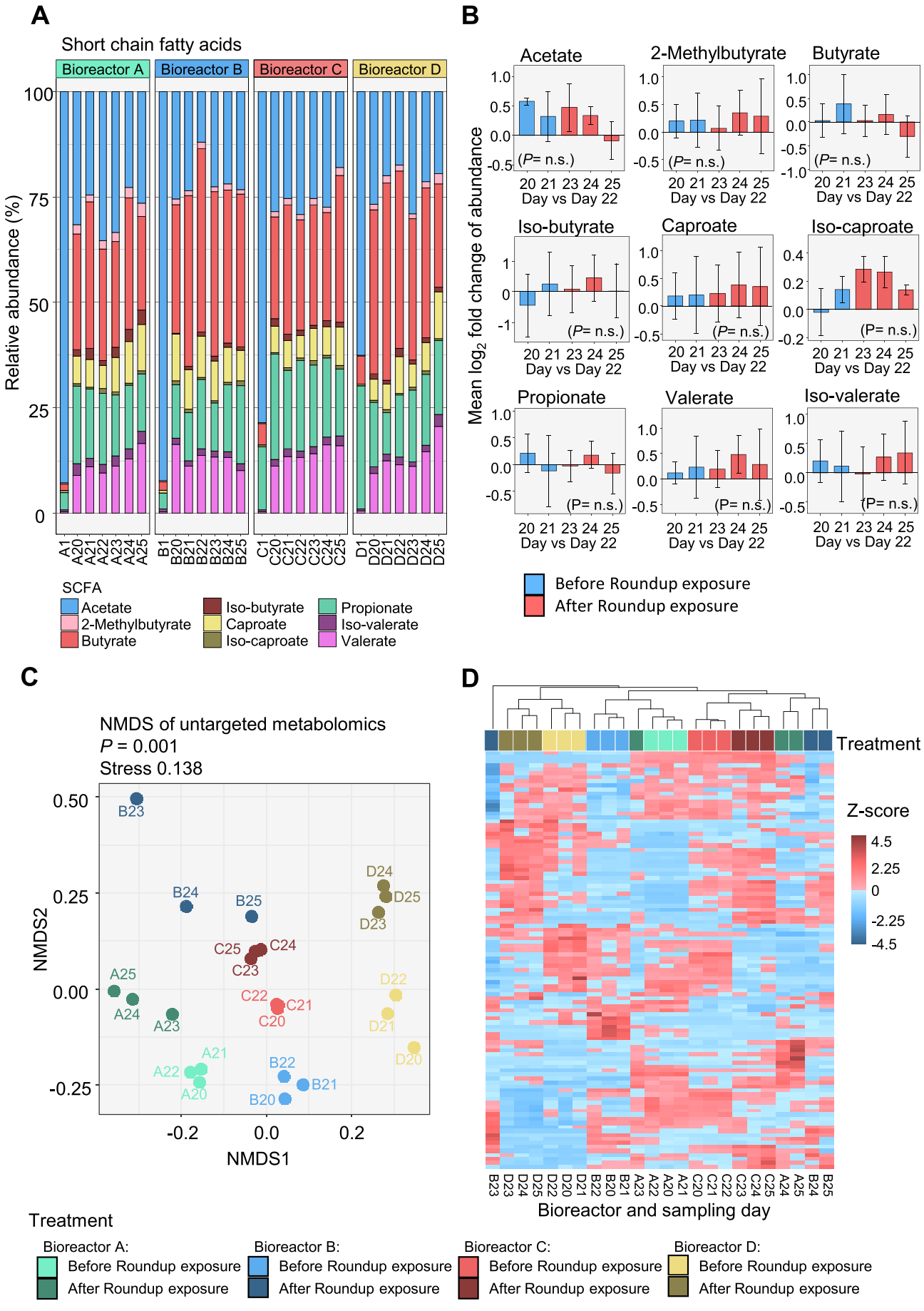
A
Short chain fatty acids
Bioreactor A
Bioreactor B
Bioreactor C
Bioreactor D
Relative abundance (%)
SCFA
Acetate
2-Methylbutyrate
Butyrate
Iso-butyrate
Caproate
Iso-caproate
Propionate
Iso-valerate
Valerate
B
Acetate
2-Methylbutyrate
Butyrate
Iso-butyrate
Caproate
Iso-caproate
Propionate
Valerate
Iso-valerate
Mean log2 fold change of abundance
(P= n.s.)
Day vs Day 22
Before Roundup exposure
After Roundup exposure
C
NMDS of untargeted metabolomics
P = 0.001
Stress 0.138
NMDS1
NMDS2
D
Treatment
Z-score
Bioreactor and sampling day
Treatment
Bioreactor A:
Before Roundup exposure
After Roundup exposure
Bioreactor B:
Before Roundup exposure
After Roundup exposure
Bioreactor C:
Before Roundup exposure
After Roundup exposure
Bioreactor D:
Before Roundup exposure
After Roundup exposure

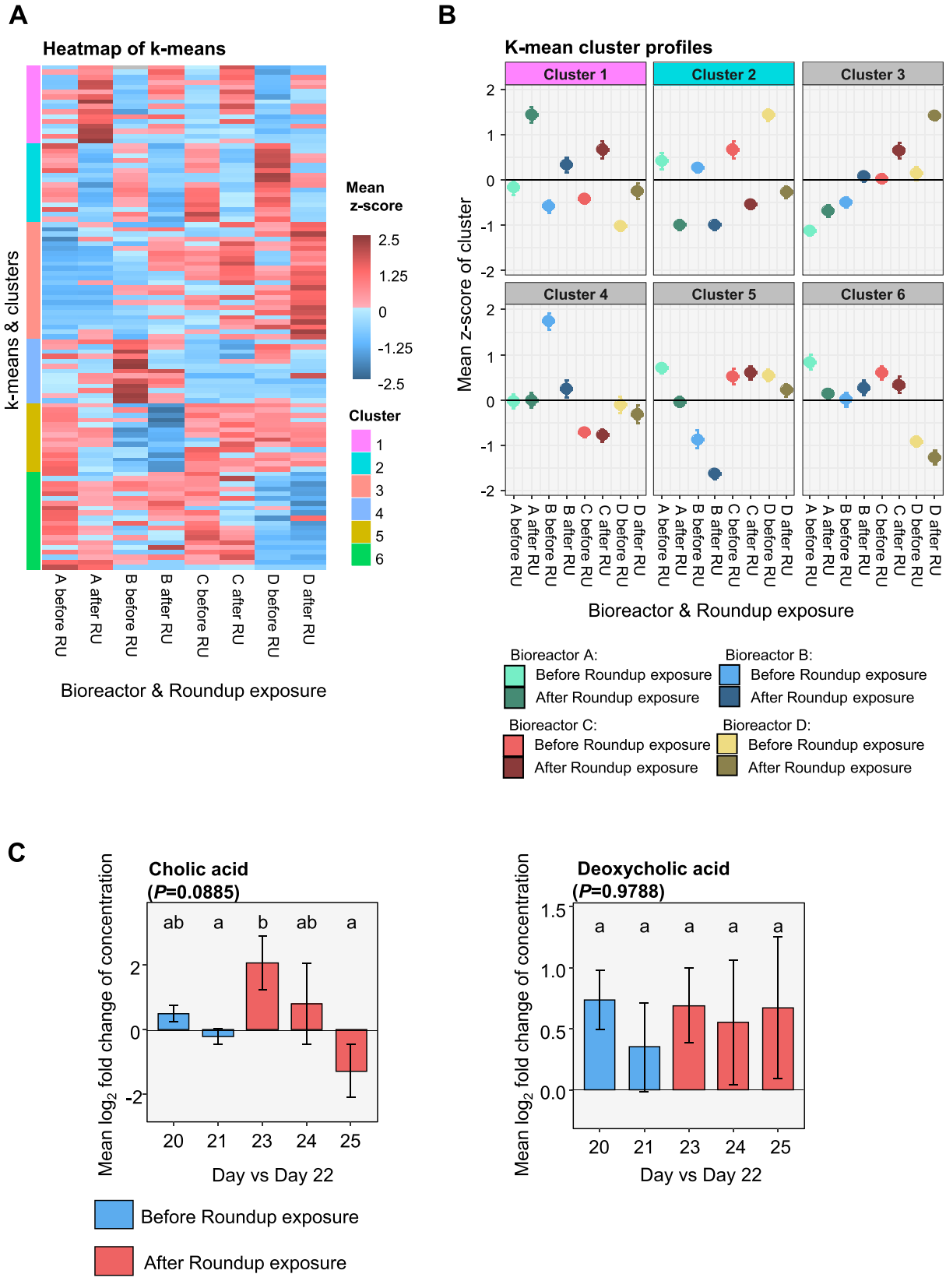

Fig. 5. Metabolomics data. **A**: K-means of peaks identified by untargeted metabolomics. **B**: Clustering profile of the k-means, only using those peaks identified in samples before and after Roundup (RU) exposure. **C**: Mean Log_2 fold changes of cholic acid concentration **D**: Mean Log_2 fold changes of deoxycholic. Bile acids were measured by targeted metabolomics and compared from each sampling day to day 22 (just before Roundup exposure). Error is SEM; P calculated by Kruskal-Wallis with pairwise posthoc test done by Dunn test.

Fig. 4. Metabolomics data. **A:** Relative abundance of short chain fatty acids (SCFAs) **B:** Mean Log_2 fold changes of SCFA absolute abundance from each sampling day to day 22 (just before Roundup exposure). Error is SEM; *P* calculated by Kruskal-Wallis with pairwise posthoc test done by Dunn test, n.s. non-significant. **C:** NMDS plot of bioreactor samples based on untargeted metabolomics with *P* calculated by PERMANOVA. **D:** Heat map of the corresponding peak intensities.

for the taxonomic alterations detected (Dechartres et al., 2019). Lozano et al. (2018) identified sex-dependent shifts in taxonomy after long-term high doses of glyphosate (2.5 g/L) from R Grand Travaux Plus exposure *via* drinking water. In this study, the chronic and high exposure to R Grand Travaux Plus might be responsible for the contrasting findings (Lozano et al., 2018). Although the exact composition of both, R Grand Travaux Plus and Roundup LB plus, are unknown, for R Grand Travaux Plus a contamination with heavy metals has been reported (Defarge et al., 2018). This, as well as potential differences in the formulation might add on to the different observations. A more recent study by Mesnage et al. (2019) investigated the effects of three different concentrations of pure glyphosate and MON 52276 on the rat microbiome for 90 days (maximal concentration of 175 mg/kg body weight). They included taxonomic and functional analysis using a multi-omics

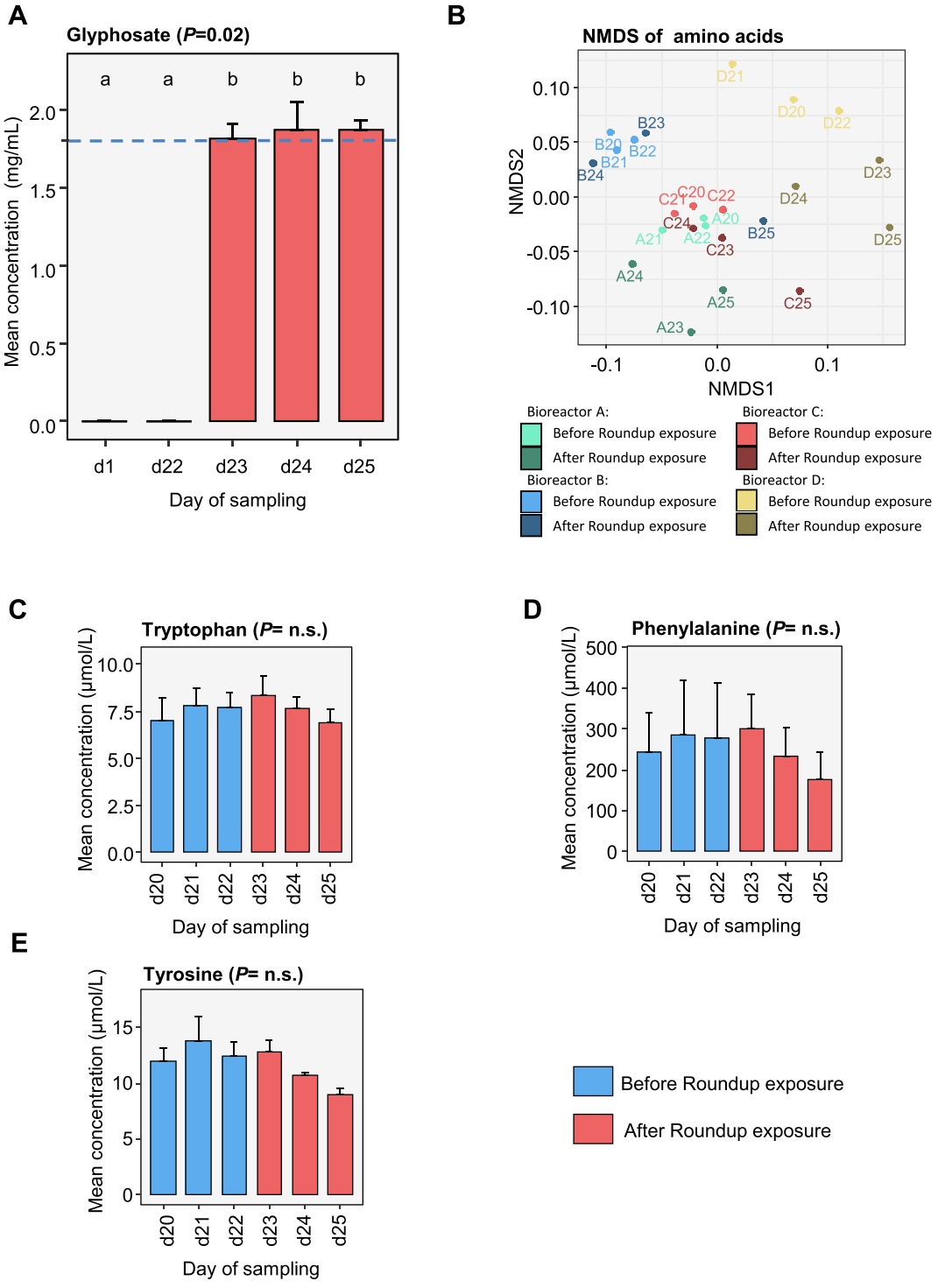

Fig. 6. Glyphosate and amino acid concentration quantified in culture medium. **A**: Detected mean glyphosate concentration with blue dotted line concentration of glyphosate (1.8 mg/mL) in the medium prepared for day 23 to day 25. When Krustal-Wallis test is significant then bars labelled with different letters are significant to each other ($P < 0.05$). **B**: NMDS-dissimilarity analysis of measured amino acid concentrations. Measured mean concentration of phenylalanine (**C**), tryptophan (**D**) and tyrosine (**E**) in samples. Error is SEM, P calculated by Kruskal-Wallis test (for amino acids P corrected for multi-testing by Benjamnini-Hochberg method) with pairwise posthoc Dunn test.

Table 1
Mean concentrations (μM) of aromatic amino acids before (days 20–22) and after Roundup exposure (days 23–25). Error is SEM.

Bioreactor	Sampling days	Phenylalanine	Tryphtophane	Tyrosine
A	20–22 (no RU)	101.8 ± 4.2	9.9 ± 0.1	12.2 ± 0.2
	23–25 (RU)	198.7 ± 10.3	9.8 ± 0.6	12.1 ± 1.2
B	20–22 (no RU)	198.3 ± 1	5.6 ± 0.2	9.7 ± 0.3
	23–25 (RU)	205.7 ± 47.5	6.8 ± 0.2	9.4 ± 0.6
C	20–22 (no RU)	143 ± 3.3	7.9 ± 0.2	12.1 ± 0.2
	23–25 (RU)	111.8 ± 34.9	7.4 ± 0.5	11.1 ± 1.5
D	20–22 (no RU)	631.3 ± 41.8	6.6 ± 0.5	16.9 ± 1.3
	23–25 (RU)	435.0 ± 45.6	6.4 ± 0.3	10.6 ± 0.4

approach. Contrary to our results, they observed slight effects on the microbial taxonomic distribution together with large inter-individual variation, which limits the reliability of the data. Alike to our study, they reported only slight effects on the metabolome in rats, with 12 of 744 metabolites being significantly altered. This corresponds to 1.6% of all metabolites. Among these metabolites, they observed an increase in shikimate and 3-dehydroshikimate, which they assigned to the inhibition of the EPSPS, the target enzyme of glyphosate from the shikimate pathway (Mesnage et al., 2019). In a further study, Nielsen et al. orally treated rats with 25 mg/kg bodyweight glyphosate or from the glyphosate formulations Glyfonova® 450 Plus for 14 days. They observed very little influence on the intestinal microbiota. The authors suggest that the availability of high concentrations of aromatic amino acids in the rat gut inhibit the synthesis of aromatic amino acids *via* the shikimate pathway. This might subsequently nullify an inhibition of the EPSPS by glyphosate (Nielsen et al., 2018), similar to our study, in which high amino acid concentrations of free amino acids were measured in pure medium. However, as Mesnage et al. (2019) indicated in their study, there may be effects on the intermediate metabolites upstream the EPSPS caused by glyphosate.

The shikimate pathway is regulated on various levels. One way of regulation is transcriptional attenuation (Pittard and Yang, 2008). A second way of regulation is negative feedback gene regulation, where the gene expression of the shikimate operon is controlled by a tryptophan sensitive (TrpR) and a tyrosine sensitive (TyrR) repressor (Pittard and Yang, 2008; Schoner and Herrmann, 1976). These repressors bind to their respective amino acid and mask the operator, thereby inhibiting transcription (Tabaka et al., 2008). Transcription inhibition commences at 10 μM of tyrosine or tryptophan, respectively (Baasov and Knowles, 1989). Another mechanism for controlling aromatic amino acid synthesis is allosteric feedback inhibition of the 3-Deoxy-D-arabinoheptulosonate 7-phosphate (DHAP) synthase. The DHAP synthase catalyzes the first enzymatic conversion in the shikimate pathway. Allosteric inhibition reaches its maximum in the presence of 100 μM of any of the aromatic amino acids (Rodriguez et al., 2014). Tyrosine and tryptophan in our study were present at concentrations, which would inhibit the DHAP synthase synthesis by transcriptional attenuation while the concentration of phenylalanine reached the concentrations where allosteric inhibition would be at maximum (see Table 1). This is in line with our finding that Roundup-exposure did not affect the abundance of protein groups of the shikimate pathway, including the EPSPS, since the medium was a model for the contents of the pig gut and therefore rich in amino acids. An inhibited shikimate pathway would result in a reduced production of aromatic amino acids, thus weakening or negating transcriptional inhibitory control. This would lead to an increase in the translation of the proteins of this pathway, which was not observed in this study. Taken together, these findings suggest that the concentrations of aromatic amino acids in the microbiota cultures were high enough to suppress the synthesis of the aromatic amino acids. The microbes were sourcing the aromatic amino acids from the media in sufficient quantities already before but also during Roundup- exposure. However, other animals, *e.g.* non-vertebrates with a less diverse microbiota or with lower aromatic amino acid levels in the gut might be susceptible to glyphosate exposure, as was proven for honey bees (Motta et al., 2018).

Since the microbial culture medium was closely modelled on the intestinal lumen content of the pig colon (Tanner et al., 2014), we would expect a similar *in vivo* response of the intestinal microbiota to Roundup-exposure as observed in our study.

5. Conclusions

An impact of the glyphosate-based herbicide Roundup® LB plus on the intestinal microbiota of pig was not confirmed at the applied glyphosate concentration. We did not observe changes on the taxonomic level and only showed minor alterations on the functional level. Nevertheless, we cannot exclude the susceptibility of microbiota in susceptible timeframes or combination with other destabilizing factors, such as medication, a shift in diet or disease. Moreover, glyphosate itself, produced glyphosate metabolites or components from the formulation after resorption from the intestine might react with other target proteins and should be included in future investigations.

CRediT authorship contribution statement

Jannike L. Krause: Conceptualization, Writing - original draft, Writing - review & editing, Formal analysis, Data curation, Investigation, Visualization. **Sven-Bastiaan Haange:** Writing - original draft, Writing - review & editing, Formal analysis, Data curation, Investigation, Software, Visualization. **Stephanie Schäpe:** Investigation, Data curation, Writing - review & editing. **Beatrice Engelmann:** Writing - review & editing, Investigation. **Ulrike Rolle-Kampczyk:** Supervision, Investigation. **Katarina Fritz-Wallace:** Writing - review & editing, Investigation. **Zhipeng Wang:** Writing - review & editing, Investigation. **Nico Jehmlich:** Conceptualization, Supervision. **Dominique Türkowsky:** Writing - review & editing. **Kristin Schubert:** Supervision. **Judith Pöppe:** Investigation. **Katrin Bote:** Investigation. **Uwe Rösler:** Funding acquisition, Writing - review & editing. **Gunda Herberth:** Supervision. **Martin von Bergen:** Conceptualization, Writing - review & editing, Supervision, Funding acquisition.

Declaration of competing interest

The authors declare that they have no known competing financial interests or personal relationships that could have appeared to influence the work reported in this paper.

Acknowledgments

Jannike Lea Krause is thankful for funding by the German Federal Environmental Foundation (DBU). Sven-Bastiaan Haange, Uwe Roesler, Judith Pöppe and Katrin Bote and Martin von Bergen are grateful for the funding by Federal Ministry of Food and Agriculture (BMEL) through the research project “Glypho-Bak” (Project number: 2815HS018). Stephanie Schäpe is grateful for support from a DFG-grant within the Priority Program 1656. We thank Florian Schattenberg for cytometric measurement of microbiota and help and discussion during data analysis. We thank Nicole Gröger and Jeremy Knespel for their excellent technical assistance and Martina Kolbe for medium supply.

Appendix A. Supplementary

Supplementary data to this article can be found online at https://doi.org/10.1016/j.scitotenv.2020.140932.

References

Amrhein, N., Schab, J., Steinrücken, H.C., 1980. The mode of action of the herbicide glyphosate. Naturwissenschaften 67, 356–357.

Authority, E.F.S., 2018. Evaluation of the impact of glyphosate and its residues in feed on animal health. EFSA J. 16, e05283.

Baasov, T., Knowles, J.R., 1989. Is the first enzyme of the shikimate pathway, 3-deoxy-D-arabino-heptulosonate-7-phosphate synthase (tyrosine sensitive), a copper metalloenzyme? J. Bacteriol. 171, 6155–6160.

Bashiardes, S., Zilberman-Schapira, G., Elinav, E., 2016. Use of metatranscriptomics in microbiome research. Bioinform Biol. Insights 10, 19–25.

Benbrook, C.M., 2016. Trends in glyphosate herbicide use in the United States and globally. Environ. Sci. Eur. 28, 3.

Benjamini, Y., Hochberg, Y., 1995. Controlling the false discovery rate - a practical and powerful approach to multiple testing. J Roy Stat Soc B Met 57, 289–300.

Brewster, D.W., Warren, J., Hopkins, W.E., 1991. Metabolism of glyphosate in Sprague-Dawley rats: tissue distribution, identification, and quantitation of glyphosate-derived materials following a single oral dose. Fundam. Appl. Toxicol. 17, 43–51.

Claus, S.P., Guillou, H., Ellero-Simatos, S., 2016. The gut microbiota: a major player in the toxicity of environmental pollutants? NPJ Biofilms Microbiomes 2, 16003.

Dechartres, J., Pawluski, J.L., Gueguen, M.M., Jablaoui, A., Maguin, E., Rhimi, M., et al., 2019. Glyphosate and glyphosate-based herbicide exposure during the peripartum period affects maternal brain plasticity, maternal behaviour and microbiome. J. Neuroendocrinol. 31, e12731.

Defarge, N., Spiroux de Vendômois, J., Séralini, G.E., 2018. Toxicity of formulants and heavy metals in glyphosate-based herbicides and other pesticides. Toxicol. Rep. 5, 156–163.

Dixon, P., 2003. VEGAN, a package of R functions for community ecology. J. Veg. Sci. 14, 927–930.

Ford, B., Bateman, L.A., Gutierrez-Palominos, L., Park, R., Nomura, D.K., 2017. Mapping proteome-wide targets of glyphosate in mice. Cell Chem. Biol. 24, 133–140.

Franzosa, E.A., Hsu, T., Sirota-Madi, A., Shafquat, A., Abu-Ali, G., Morgan, X.C., et al., 2015. Sequencing and beyond: integrating molecular 'omics' for microbial community profiling. Nat. Rev. Microbiol. 13, 360–372.

Fritz-Wallace, K., Engelmann, B., Krause, J.L., Schape, S.S., Poppe, J., Herberth, G., et al., 2020. Quantification of glyphosate and aminomethylphosphonic acid from microbiome reactor fluids. Rapid Commun. Mass Spectrom. 34, e8668.

Funke, T., Yang, Y., Han, H., Healy-Fried, M., Olesen, S., Becker, A., et al., 2009. Structural basis of glyphosate resistance resulting from the double mutation Thr97 → Ile and Pro101 → Ser in 5-enolpyruvylshikimate-3-phosphate synthase from Escherichia coli. J. Biol. Chem. 284, 9854–9860.

Haange, S.B., Jehmlich, N., Hoffmann, M., Weber, K., Lehmann, J., von Bergen, M., et al., 2019. Disease development is accompanied by changes in bacterial protein abundance and functions in a refined model of dextran sulfate sodium (DSS)-induced colitis. J. Proteome Res. 18, 1774–1786.

Haange, S.-B., Jehmlich, N., Krügel, U., Hintschich, C., Wehrmann, D., Hankir, M., et al., 2020. Gastric bypass surgery in a rat model alters the community structure and functional composition of the intestinal microbiota independently of weight loss. Microbiome 8, 13.

Hanke, I., Wittmer, I., Bischofberger, S., Stamm, C., Singer, H., 2010. Relevance of urban glyphosate use for surface water quality. Chemosphere 81, 422–429.

Heintz-Buschart, A., Wilmes, P., 2018. Human gut microbiome: function matters. Trends Microbiol. 26, 563–574.

Hugenholtz, F., de Vos, W.M., 2018. Mouse models for human intestinal microbiota research: a critical evaluation. Cellular Mol. Life Sci. 75, 149–160.

Ihaka, R., Gentleman, R., 1996. R: a language for data analysis and graphics. J. Comput. Graph. Stat. 5, 299–314.

Islam, K.B., Fukiya, S., Hagio, M., Fujii, N., Ishizuka, S., Ooka, T., et al., 2011. Bile acid is a host factor that regulates the composition of the cecal microbiota in rats. Gastroenterology 141, 1773–1781.

Joly, C., Gay-Queheillard, J., Leke, A., Chardon, K., Delanaud, S., Bach, V., et al., 2013. Impact of chronic exposure to low doses of chlorpyrifos on the intestinal microbiota in the simulator of the human intestinal microbial ecosystem (SHIME) and in the rat. Environ. Sci. Pollut. Res. Int. 20, 2726–2734.

Kanehisa, M., Goto, S., 2000. KEGG: Kyoto encyclopedia of genes and genomes. Nucleic Acids Res. 28, 27–30.

Kleiner, M., Thorson, E., Sharp, C.E., Dong, X., Liu, D., Li, C., et al., 2017. Assessing species biomass contributions in microbial communities via metaproteomics. Nat. Commun. 8, 1558.

Koch, C., Fetzer, I., Schmidt, T., Harms, H., Muller, S., 2013. Monitoring functions in managed microbial systems by cytometric bar coding. Environ. Sci. Technol. 47, 1753–1760.

Krause, J.L., Schaepe, S.S., Fritz-Wallace, K., Engelmann, B., Rolle-Kampczyk, U., Kleinsteuber, S., et al., 2020. Following the community development of SIHUMIx – a new intestinal in vitro model for bioreactor use. Gut Microbes 1–14.

Lagkouvardos, I., Fischer, S., Kumar, N., Clavel, T., 2017. Rhea: a transparent and modular R pipeline for microbial profiling based on 16S rRNA gene amplicons. Peerj 5, e2836.

Levy, M., Kolodziejczyk, A.A., Thaiss, C.A., Elinav, E., 2017. Dysbiosis and the immune system. Nat. Rev. Immunol. 17, 219–232.

Li, L., Abou-Samra, E., Ning, Z., Zhang, X., Mayne, J., Wang, J., et al., 2019. An in vitro model maintaining taxon-specific functional activities of the gut microbiome. Nat. Commun. 10, 4146.

Licht, T.R., Bahl, M.I., 2019. Impact of the gut microbiota on chemical risk assessment. Curr. Opin. Toxicol. 15, 109–113.

Liu, L., Firrman, J., Tanes, C., Bittinger, K., Thomas-Gahring, A., Wu, G.D., et al., 2018. Establishing a mucosal gut microbial community in vitro using an artificial simulator. PLoS One 13, e0197692.

Lohmann, P., Schäpe, S.S., Haange, S.-B., Oliphant, K., Allen-Vercoe, E., Jehmlich, N., et al., 2020. Function is what counts: how microbial community complexity affects species, proteome and pathway coverage in metaproteomics. Expert Rev. Proteom. 17, 163–173.

Lozano, V.L., Defarge, N., Rocque, L.-M., Mesnage, R., Hennequin, D., Cassier, R., et al., 2018. Sex-dependent impact of Roundup on the rat gut microbiome. Toxicol. Rep. 5, 96–107.

Lozupone, C.A., Stombaugh, J.I., Gordon, J.I., Jansson, J.K., Knight, R., 2012. Diversity, stability and resilience of the human gut microbiota. Nature 489, 220–230.

Macpherson, A.J., McCoy, K.D., 2015. Standardised animal models of host microbial mutualism. Mucosal Immunol. 8, 476–486.

McNeil, B., Harvey, L.M., 2008. Fermentation: An art from the past, a skill for the future. In: McNeil, B., Harvey, L.M. (Eds.), Practical Fermentation Technology, pp. 1–2.

Medicine Io, 2003. Microbial Threats to Health: Emergence, Detection, and Response. The National Academies Press, Washington, DC.

Mesnage, R., Antoniou, M.N., 2017. Ignoring adjuvant toxicity falsifies the safety profile of commercial pesticides. Front. Public Health 5, 361.

Mesnage, R., Arno, M., Costanzo, M., Malatesta, M., Seralini, G.E., Antoniou, M.N., 2015. Transcriptome profile analysis reflects rat liver and kidney damage following chronic ultra-low dose Roundup exposure. Environ. Health 14, 70.

Mesnage, R., Teixeira, M., Mandrioli, D., Falcioni, L., Ducarmon, Q.R., Zwittink, R.D., et al., 2019. Shotgun Metagenomics and Metabolomics Reveal Glyphosate Alters the Gut Microbiome of Sprague-Dawley Rats by Inhibiting the Shikimate Pathway. bioRxiv. p. 870105.

Motta, E.V.S., Raymann, K., Moran, N.A., 2018. Glyphosate perturbs the gut microbiota of honey bees. Proc. Natl. Acad. Sci. 201803880.

Mumtaz, M.W., Hamid, A.A., Akhtar, M.T., Anwar, F., Rashid, U., Al-Zuaidy, M.H., 2017. An overview of recent developments in metabolomics and proteomics – phytotherapic research perspectives. Frontiers in Life Science 10, 1–37.

Myers, J.P., Antoniou, M.N., Blumberg, B., Carroll, L., Colborn, T., Everett, L.G., et al., 2016. Concerns over use of glyphosate-based herbicides and risks associated with exposures: a consensus statement. Environ. Health 15, 19.

Nielsen, L.N., Roager, H.M., Casas, M.E., Frandsen, H.L., Gosewinkel, U., Bester, K., et al., 2018. Glyphosate has limited short-term effects on commensal bacterial community composition in the gut environment due to sufficient aromatic amino acid levels. Environ. Pollut. 233, 364–376.

Payne, A.N., Zihler, A., Chassard, C., Lacroix, C., 2012. Advances and perspectives in in vitro human gut fermentation modeling. Trends Biotechnol. 30, 17–25.

Pittard, J., Yang, J., 2008. Biosynthesis of the aromatic amino acids. EcoSal Plus 3.

Priestman, M.A., Funke, T., Singh, I.M., Crupper, S.S., Schonbrunn, E., 2005. 5-Enolpyruvylshikimate-3-phosphate synthase from Staphylococcus aureus is insensitive to glyphosate. FEBS Lett. 579, 728–732.

Qin, J., Li, R., Raes, J., Arumugam, M., Burgdorf, K.S., Manichanh, C., et al., 2010. A human gut microbial gene catalogue established by metagenomic sequencing. Nature 464, 59–65.

Quast, C., Pruesse, E., Yilmaz, P., Gerken, J., Schweer, T., Yarza, P., et al., 2013. The SILVA ribosomal RNA gene database project: improved data processing and web-based tools. Nucleic Acids Res. 41, D590–D596.

Riede, S., Toboldt, A., Breves, G., Metzner, M., Kohler, B., Braunig, J., et al., 2016. Investigations on the possible impact of a glyphosate-containing herbicide on ruminal metabolism and bacteria in vitro by means of the 'Rumen simulation technique'. J. Appl. Microbiol. 121, 644–656.

Rodriguez, A., Martinez, J.A., Flores, N., Escalante, A., Gosset, G., Bolivar, F., 2014. Engineering Escherichia coli to overproduce aromatic amino acids and derived compounds. Microb. Cell Factories 13, 126.

Roura, E., Koopmans, S.J., Lalles, J.P., Le Huerou-Luron, I., de Jager, N., Schuurman, T., et al., 2016. Critical review evaluating the pig as a model for human nutritional physiology. Nutr. Res. Rev. 29, 60–90.

Ryan, K.K., Tremaroli, V., Clemmensen, C., Kovatcheva-Datchary, P., Myronovych, A., Karns, R., et al., 2014. FXR is a molecular target for the effects of vertical sleeve gastrectomy. Nature 509, 183–188.

Savitski, M.M., Reinhard, F.B.M., Franken, H., Werner, T., Savitski, M.F., Eberhard, D., et al., 2014. Tracking cancer drugs in living cells by thermal profiling of the proteome. Science 346, 1255784.

Schape, S.S., Krause, J.L., Engelmann, B., Fritz-Wallace, K., Schattenberg, F., Liu, Z., et al., 2019. The simplified human intestinal microbiota (SIHUMIx) shows high structural and functional resistance against changing transit times in in vitro bioreactors. Microorganisms 7.

Schoner, R., Herrmann, K.M., 1976. 3-Deoxy-D-arabino-heptulosonate 7-phosphate synthase. Purification, properties, and kinetics of the tyrosine-sensitive isoenzyme from Escherichia coli. J. Biol. Chem. 251, 5440–5447.

Shamir, M., Bar-On, Y., Phillips, R., Milo, R., 2016. SnapShot: timescales in cell biology. Cell 164, 1302–e1.

Shehata, A.A., Schrodl, W., Aldin, A.A., Hafez, H.M., Kruger, M., 2013. The effect of glyphosate on potential pathogens and beneficial members of poultry microbiota in vitro. Curr. Microbiol. 66, 350–358.

Siskos, A.P., Jain, P., Romisch-Margl, W., Bennett, M., Achaintre, D., Asad, Y., et al., 2017. Interlaboratory reproducibility of a targeted metabolomics platform for analysis of human serum and plasma. Anal. Chem. 89, 656–665.

Tabaka, M., Cybulski, O., Holyst, R., 2008. Accurate genetic switch in Escherichia coli: novel mechanism of regulation by co-repressor. J. Mol. Biol. 377, 1002–1014.

Tanner, S.A., Zihler Berner, A., Rigozzi, E., Grattepanche, F., Chassard, C., Lacroix, C., 2014. In vitro continuous fermentation model (PolyFermS) of the swine proximal colon for simultaneous testing on the same gut microbiota. PLoS One 9, e94123.

Tarazona, J.V., Court-Marques, D., Tiramani, M., Reich, H., Pfeil, R., Istace, F., et al., 2017. Glyphosate toxicity and carcinogenicity: a review of the scientific basis of the European Union assessment and its differences with IARC. Arch. Toxicol. 91, 2723–2743.

Tsiaoussis, J., Antoniou, M.N., Koliarakis, I., Mesnage, R., Vardavas, C.I., Izotov, B.N., et al., 2019. Effects of single and combined toxic exposures on the gut microbiome: current knowledge and future directions. Toxicol. Lett. 312, 72–97.

Türkowsky, D., Lohmann, P., Mühlenbrink, M., Schubert, T., Adrian, L., Goris, T., et al., 2019. Thermal proteome profiling allows quantitative assessment of interactions between tetrachloroethene reductive dehalogenase and trichloroethene. J. Proteome 192, 10–17.

Turnbaugh, P.J., Ley, R.E., Hamady, M., Fraser-Liggett, C.M., Knight, R., Gordon, J.I., 2007. The human microbiome project. Nature 449, 804–810.

von Bergen, M., Jehmlich, N., Taubert, M., Vogt, C., Bastida, F., Herbst, F.A., et al., 2013. Insights from quantitative metaproteomics and protein-stable isotope probing into microbial ecology. ISME J 7, 1877–1885.

Wickham, H., 2011. ggplot2. Wiley Interdiscip. Rev. Comput. Stat. 3, 180–185.

Wilfart, A., Montagne, L., Simmins, H., Noblet, J., Milgen, J., 2007. Digesta transit in different segments of the gastrointestinal tract of pigs as affected by insoluble fibre supplied by wheat bran. Br. J. Nutr. 98, 54–62.

Xu, J., 2006. Microbial ecology in the age of genomics and metagenomics: concepts, tools, and recent advances. Mol. Ecol. 15, 1713–1731.

Yadav, M., Verma, M.K., Chauhan, N.S., 2018. A review of metabolic potential of human gut microbiome in human nutrition. Arch. Microbiol. 200, 203–217.

Yan, A.W., Fouts, D.E., Brandl, J., Starkel, P., Torralba, M., Schott, E., et al., 2011. Enteric dysbiosis associated with a mouse model of alcoholic liver disease. Hepatology 53, 96–105.

Yokota, A., Fukiya, S., Islam, K.B.M.S., Ooka, T., Ogura, Y., Hayashi, T., et al., 2012. Is bile acid a determinant of the gut microbiota on a high-fat diet? Gut Microbes 3, 455–459.